



Surfactant effects on water recovery from produced water via direct-contact membrane distillation



Nick Guan Pin Chew^{a,b}, Shanshan Zhao^b, Chun Heng Loh^b, Nadia Permogorov^c, Rong Wang^{b,d,*}

^a Interdisciplinary Graduate School, Nanyang Technological University, Singapore 639798, Singapore

^b Singapore Membrane Technology Centre, Nanyang Environment and Water Research Institute, Nanyang Technological University, Singapore 637141, Singapore

^c Johnson Matthey Technology Centre, Reading RG4 9NH, United Kingdom

^d School of Civil and Environmental Engineering, Nanyang Technological University, Singapore 639798, Singapore

ARTICLE INFO

Keywords:

Membrane distillation
Produced water
Surfactant
Oil-in-water emulsion
Water recovery

ABSTRACT

Increasing demand for oil and gas leads to the generation of substantial amount of produced water, bringing about deleterious impacts on the environment. Direct-contact membrane distillation (DCMD) could be a possible option for dewatering oil-in-water (O/W) emulsions because of many benefits brought by the DCMD process. However, these low surface tension solutions pose some difficult issues such as membrane fouling and pore wetting. The mechanisms involved are not fully understood due to the lack of study of the interaction between the emulsions and the membrane surface in the DCMD domain. To address the challenges, this study aims at developing a fundamental understanding of the relationship between surfactant-stabilized O/W emulsions and polyvinylidene fluoride (PVDF) membrane surface in DCMD operations. Effects of surfactant types (Span 20, Tween 20, and sodium dodecyl sulfate), oil concentration, and oil types (petroleum and vacuum pump oil) were systematically studied to better understand the fouling and wetting mechanisms involved. The results reveal that surfactant concentration and hydrophobicity had an influence on the membrane fouling and wetting behaviors. Surfactants with a lower hydrophilic-lipophilic balance (HLB) value could make the PVDF membrane surface less hydrophobic and cause less severe fouling by restraining the adsorption of oil droplets on the membrane surface. These findings suggest that membrane surface modification is required to achieve anti-fouling and anti-wetting properties to make DCMD an energy-efficient and effective technology for treating produced water.

1. Introduction

Produced water is wastewater co-produced in a producing well along with the oil and/or gas phase(s) [1]. It is commonly known as the largest waste stream from the oil and gas refineries as it contains a variety of pollutants, namely: (i) dissolved and dispersed oils and greases; (ii) production solids; (iii) dissolved gases; (iv) soluble and insoluble organics; (v) production chemicals; (vi) inorganics and (vii) dissolved formation minerals [2]. These constituents of produced water are highly dependent on the geological locations as well as formation processes. As the demand for oil and gas is expected to rise even further in the next couple of decades, the generation of produced water is showing no signs of slowing down [3]. The oil and gas industries are thus facing a grand challenge – huge quantities of wastewater. Therefore, it is of paramount importance to develop effective manage-

ment strategies for produced water.

Generally, several options are available for produced water management: (i) injection of the produced water into the same formation process or another suitable formation; (ii) discharge back into the environment after treatment; (iii) reuse in oil and gas field operations after treatment; and (iv) beneficial reuse for consumption or agricultural purposes after treatment [4]. Currently, industries are placing more emphasis on the treatment and reuse of produced water mainly due to the stringent environmental regulations, increased pressure on water resources, and the rising cost of wastewater discharge. However, the conventional treatment methods often have several intrinsic disadvantages, including low removal efficiencies of oil droplets with diameters less than 20 μm , low water recovery, high operation costs as well as the possibility of corrosion and recontamination [5]. The rapid development of membrane technologies offers attractive solutions to

* Corresponding author at: Singapore Membrane Technology Centre, Nanyang Environment and Water Research Institute, Nanyang Technological University, Singapore 637141, Singapore.

E-mail address: rwang@ntu.edu.sg (R. Wang).

<http://dx.doi.org/10.1016/j.memsci.2017.01.024>

Received 29 October 2016; Received in revised form 15 January 2017; Accepted 16 January 2017

Available online 17 January 2017

0376-7388/ © 2017 Elsevier B.V. All rights reserved.

produced water treatment. Over the past few decades, membrane processes such as microfiltration (MF) [6–8], ultrafiltration (UF) [9–11], nanofiltration (NF) [12–14], reverse osmosis (RO) [15,16], and forward osmosis (FO) [17] have been applied for produced water treatment. These membrane technologies have been preferred over the conventional methods due to their high oil removal efficiencies, small footprint, and easy operation and maintenance. While some of these processes can be combined to achieve high removal efficiencies, high operating costs remain a major concern. Another grand challenge is membrane fouling caused by oil droplets and soluble organics.

Membrane distillation (MD), which is an emerging technology that can utilize low-grade waste heat to generate high quality water, offers a possible solution. In MD, water vapor from the higher temperature feed side is transported through a porous hydrophobic membrane and condensed on the lower temperature permeate side, driven by the vapor pressure difference across the membrane caused by the temperature gradient [18]. MD is favored for the dewatering of produced water due to its moderate operating conditions, lower operating hydrostatic pressure, theoretically complete removal of non-volatiles and high recovery amongst other benefits [19]. Its main advantage over other membrane processes is its capability for utilizing low-grade waste heat, which is abundant in oil and gas refineries. This could potentially reduce the energy costs for the MD process. Among four different types of configuration, the direct-contact membrane distillation (DCMD) is widely studied due to its simple operation mode [20].

Over the past decade, numerous studies have been conducted on the application of MD for the treatment of oily wastewater and produced water [4,21–25]. The influences of pretreatment, operation conditions, and novel membrane surface modifications have been intensively studied. In most of these works, different pretreatment techniques were used to remove oil before the MD stage. Therefore, the true potential of MD in the treatment of produced water has not been explored. In particular, very limited amount of work has been reported on the influences of surfactants on membrane fouling and pore wetting. In produced water, oil is typically emulsified by the existence of natural or added surfactants, which can significantly reduce the pore liquid entry pressure (LEP) of MD membranes, leading to the penetration of feed water into the permeate stream, consequently resulting in the failure of the MD operation.

This study aims at developing a fundamental understanding of the relationship between surfactant-stabilized O/W emulsions and polyvinylidene fluoride (PVDF) membrane surface in the DCMD process. A PVDF membrane was selected because it is hydrophobic in nature, which is a fundamental requirement for MD operations. Specifically, a series of bench-scale experiments were conducted to investigate on the roles of different types and concentrations of oil and surfactant on the fouling and wetting behaviors of the PVDF membrane. Membrane autopsy was also conducted using Fourier transform infrared spectroscopy (FTIR) and field emission scanning electron microscopy (FE-SEM) to confirm the wetting and fouling phenomena in the DCMD process. It is expected that this study can provide guidance for developing new strategies to facilitate DCMD as an energy-efficient and effective technology for treating produced water.

2. Experimental

2.1. Chemicals

Sodium chloride (NaCl, 99.5%), Span 20, Tween 20, and sodium dodecyl sulfate (SDS) were purchased from Merck Millipore. The reagents were used as received. Petroleum and vacuum pump oil (VPO) were purchased from Sigma-Aldrich and used without any treatment. The properties of oils and surfactants used in this study are presented in Table 1 and Table 2, respectively. Milli-Q water was produced by the Millipore Water Purification System.

Table 1
Properties of oils used in this study.

Oil type	Relative density (g ml ⁻¹)	Boiling point (K)	Flash point (K)	Components
Petroleum	0.79	453–493	334	~18% aromatics
VPO	0.88	662	523	Solvent-refined heavy paraffinic

2.2. Characteristics of PVDF hollow fiber membrane

PVDF hollow fiber membranes were supplied by a commercial manufacturer. The relevant membrane properties were characterized and summarized in Table 3. Lab-scale modules were prepared by sealing 10 pieces of 18 cm long hollow fiber in Teflon tubing. A new membrane module was used for each experiment. The effective membrane area for each module was 87 cm².

2.3. Preparation and characterization of surfactant-stabilized O/W emulsions

8 L of synthetic produced water was formulated using predetermined concentrations of oil, surfactant, and NaCl. Oil and surfactant were mixed at 9:1 mass ratio in Milli-Q water to mimic produced water. It also contained 3.5 wt% NaCl to represent the total dissolved solids (TDS). The surfactant-stabilized O/W emulsions were obtained by mixing the solutions using a heavy-duty blender (Waring® Commercial, USA) at a high speed for at least 3 min. The conductivities of the emulsions were measured to be around 50 mS cm⁻¹.

The oil droplet sizes of the emulsions were measured by a Mastersizer (Hydro 2000SM, Malvern Instruments, UK). The zeta potentials of the emulsions were measured by a Zetasizer (Nano ZS, Malvern Instruments, UK).

2.4. DCMD experiment

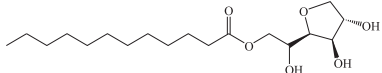
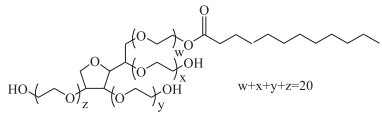
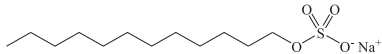
The DCMD experimental rig used for the experiments has been illustrated in our previous work [28]. The feed solutions were heated and maintained at 333 K and circulated on the shell side of the hollow fiber membranes. The permeate water was cooled and maintained at 293 K and circulated in the lumen side of the hollow fiber membranes in a countercurrent flow to the feed. The feed and permeate volumetric flow rates were maintained at 0.7 L min⁻¹ and 0.25 L min⁻¹ respectively, corresponding to Reynolds numbers of 1631 and 609 respectively. A higher flow rate was employed on the feed side to mitigate concentration and temperature polarizations [28]. The permeate overflow was collected into a tank. The permeate flux was measured and recorded every minute after the experimental conditions were stabilized (approx. 1 h). Throughout the entire duration of the MD experiments, the tubes and membrane modules were insulated to minimize heat loss.

2.5. Characterization tests

An in-house-made LEP experimental setup was used for the measurement of LEP_w of the pristine PVDF membrane as described in our previous research [29]. The mechanical properties of the membrane were measured by a Zwick Roell BT1-FR0.5TN.D14 Material Testing Machine at a constant elongation velocity of 50 mm min⁻¹ under room temperature. The mean pore size and pore size distribution of the membrane were determined by a capillary flow porometer (CFP 1500A, Porous Material, Inc., USA). The membrane porosity was calculated by dividing the volume of pores by the total volume of the membrane as described in our previous research [29].

The presence of surfactants on the inner surfaces of the membranes

Table 2
Properties of surfactants used in this study.

Surfactant	Molecular weight (g mol ⁻¹)	HLB ^a	CMC ^b (mg L ⁻¹)	Surface tension ^c (mN m ⁻¹)	Chemical structure
Span 20	346.5	8.6 [26]	1.6	~25	
Tween 20	1227.5	16.7 [26]	3.5	~31	
SDS	288.4	40.0 [27]	129	~40	

^a Hydrophilic-lipophilic balance.

^b Critical micelle concentration (in 3.5 wt% NaCl at 333 K).

^c Surface tension was measured at 0.15 mM in 3.5 wt% NaCl.

Table 3
PVDF membrane properties.

Dimension (mm)	Pore size (μm)	Contact angle, θ (°)	Porosity, ε (%)	LEP _w ^a (bar)	Tensile modulus, E _t (MPa)	Strain, δ _b (%)	Zeta potential ^b (mV)
d ₀ : 1.531 d _i : 0.872	r _{max} : 0.183 r _{mean} : 0.022	116	83	3.14	26.4	126.6	-52.5

^a Water liquid entry pressure.

^b Surface zeta potential was measured in NaCl solution at pH 7.

was detected using a Fourier transform infrared spectroscopy via the attenuated total reflectance mode (ATR-FTIR) (IR-Prestige-21 spectrophotometer, Shimadzu, Japan). The FTIR spectra were collected at room temperature over a scanning range of 400–4000 cm⁻¹ with a resolution of 4 cm⁻¹. The Happ-Genzel function was selected as the apodization function. The outer surface morphologies of the pristine and fouled PVDF membranes were observed through a FE-SEM (JEOL JSM-7600F, USA). The hollow fibers were sputter coated with platinum prior to the respective tests.

The dynamic contact angles of the virgin and used PVDF membranes were determined by a tensiometer (DCAT11, Data Physics Corporation, USA). A hollow fiber sample glued to a holder was hung from the arm of an electro-balance and underwent through three cycles of immersion (surface detection threshold at 0.5 mg) into Milli-Q water at an immersion depth of 5 mm. The dynamic contact angles were calculated from the wetting force according to the Wilhelmy method. Each membrane sample was measured ten times and an average value was calculated. The surface zeta potential of the PVDF membrane was determined using an electrokinetic analyzer (SurPASSTM 3, Anton Paar, Austria) based on streaming potential measurements. 1 mM NaCl was prepared as the background electrolyte solution. 0.05 M HCl and NaOH were used for pH titration. The resulting potential difference was detected and calculated using the Helmholtz-Smoluchowski equation.

The critical micelle concentration (CMC) values of the respective surfactants were also determined by the tensiometer. Predetermined concentrations of surfactant solutions were prepared and injected into a dish that contained 3.5 wt% NaCl solution, which was maintained at 333 K by a recirculating water bath. The changes in the surface tension of the NaCl solution were measured. CMC was reached when the surface tension remained relatively constant. Each CMC value was measured three times and an average value was obtained.

3. Results and discussion

3.1. Oil droplet sizes and zeta potentials of surfactant-stabilized O/W emulsions

Three types of surfactant commonly used in the petroleum industry (Span 20, Tween 20, and SDS) and two types of oil (petroleum and VPO) were used to prepare the surfactant-stabilized O/W emulsions [30]. These O/W emulsions were modeled as similar to real oilfield-produced water samples as possible, which generally contain 2–565 mg L⁻¹ of oil [2]. The mean droplet sizes and zeta potentials of these emulsions are listed in Table 4. The oil droplet size distributions of the emulsions are presented in Fig. 1. Oilfield-produced water typically has oil droplet sizes ranging from 2 to 30 μm [11]. However,

Table 4
Number average mean droplet size, span of distribution, and zeta potential of the surfactant-stabilized O/W emulsions.

Composition	Mean droplet size ^a (μm)	Span of distribution ^b	Zeta potential (mV)
500 mg L ⁻¹ Span 20/ Petroleum Emulsion	7.74	2.05	-3.36 ± 0.44
500 mg L ⁻¹ Tween 20/ Petroleum Emulsion	2.16	2.82	-3.11 ± 0.32
500 mg L ⁻¹ SDS/ Petroleum Emulsion	3.48	1.74	-37.2 ± 1.1
500 mg L ⁻¹ Tween 20/ VPO Emulsion	7.27	2.24	-3.38 ± 0.12
600 mg L ⁻¹ Tween 20/ Petroleum Emulsion	2.39	2.84	N.A ^c
1000 mg L ⁻¹ Tween 20/ Petroleum Emulsion	2.64	2.85	N.A ^c

^a Mean droplet size was measured when the feed solution was heated up to 333 K.

^b The larger the span of distribution is, the more polydisperse the emulsion.

^c Not applicable. The zeta potentials of these emulsions were not measured.

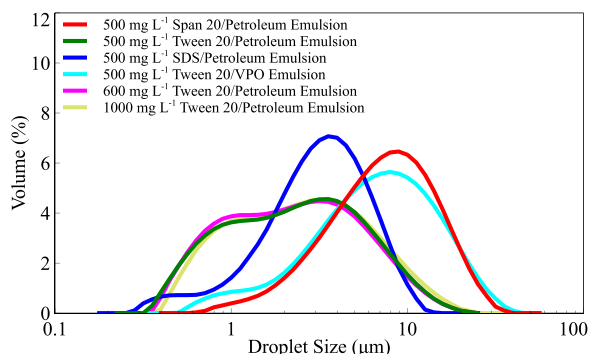


Fig. 1. Oil droplet size distributions of different O/W emulsions.

the oil droplet sizes of all the emulsions were kept below 10 μm to form kinetically stable O/W emulsions [31]. It can be seen that the mean droplet size was dependent on the types of oil and surfactant. With the same oil/surfactant mass ratio and stirring time, the petroleum emulsion stabilized by Span 20 had a larger mean oil droplet size as compared to other surfactants because oil droplets have a greater tendency to coalesce in this case. When comparing different types of oil stabilized by the same surfactant (Tween 20 in this case), the oil droplet size of the VPO emulsion was larger than that of the petroleum emulsion due to the higher proportion of heavy hydrocarbons present in VPO [32]. According to the measured zeta potentials, the Span 20 and Tween 20-stabilized emulsions were nearly neutral while the SDS-stabilized emulsion was negatively charged.

3.2. Effects of surfactant types

A baseline test was first conducted using 3.5 wt% NaCl as the feed solution, which represented the TDS present in produced water. The purpose of running a baseline test was to ascertain that the addition of NaCl did not contribute to changes in the permeate flux and conductivity, if any. As shown in Fig. 2, the permeate flux was steady and observed to be approximately 11 kg m⁻² h⁻¹ while the permeate conductivity was fairly constant throughout, ranging between 2–3 μS cm⁻¹. This suggests that scaling and wetting did not take place during the experiment.

Fig. 3 shows the effects of different surfactants on the permeate flux and conductivity during the MD process. To ensure a fair comparison, the same molar concentration of surfactant was used. From Fig. 3, a significant rise in the permeate conductivities was observed, demonstrating the wetting of membrane during the MD process. The time for the onset of wetting was defined as the time when the permeate conductivity increased by 1 μS cm⁻¹ due to the diffusion of NaCl into

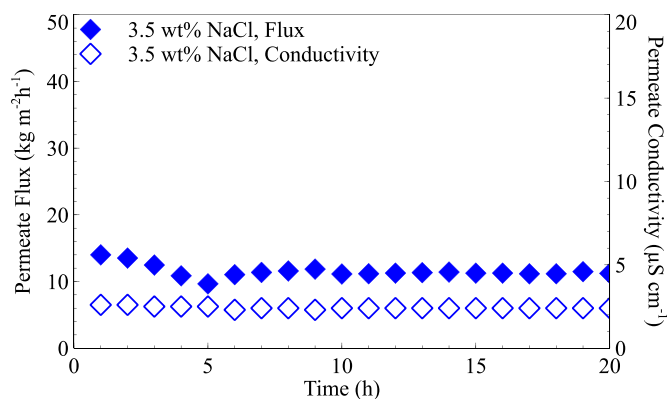


Fig. 2. Effects of 3.5 wt% NaCl solution on permeate flux (filled symbols) and conductivity (hollow symbols). (Feed volumetric flow rate (Q_f)=0.7 L min⁻¹; Permeate volumetric flow rate (Q_p)=0.25 L min⁻¹; Feed temperature (T_f)=333 K; Permeate temperature (T_p)=293 K).

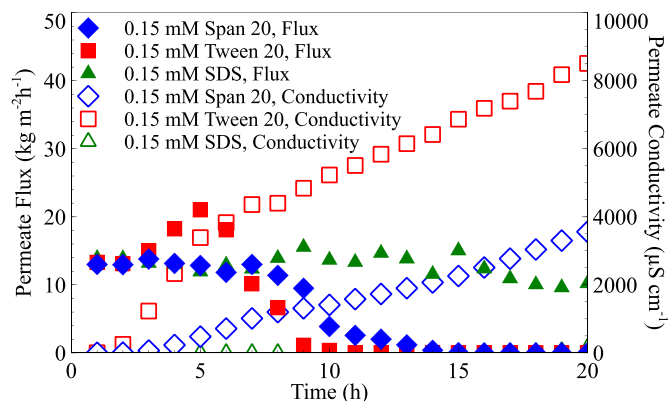


Fig. 3. Effects of surfactant types (same molar concentration) on permeate flux (filled symbols) and conductivity (hollow symbols). (Q_f =0.7 L min⁻¹; Q_p =0.25 L min⁻¹; T_f =333 K; T_p =293 K).

Table 5

Wetting time, final permeate conductivity, and contact angle of surfactant-fouled membranes in DCMD using feed with different surfactants.

Membrane	Time for onset of wetting (min)	Final permeate conductivity (mS cm ⁻¹)	Contact angle (°)
No surfactant	–	–	116 ± 2
0.15 mM Span 20	~105	3.56	72 ± 3
0.15 mM Tween 20	~70	8.51	64 ± 2
0.15 mM SDS	~520	0.15	91 ± 1
50 mg L ⁻¹ Span 20	~100	3.69	72 ± 1
50 mg L ⁻¹ Tween 20	~130	12.55	63 ± 1
50 mg L ⁻¹ SDS	~140	0.95	85 ± 1

the permeate side. The wetting times and the final permeate conductivities in different surfactant experiments are listed in Table 5. The results show that Tween 20 exhibited the earliest wetting with an onset of wetting occurring at ~70 min, followed by Span 20 (~105 min), and SDS (~520 min). The severity of membrane wetting was in the sequence of Tween 20 > Span 20 > SDS as well, and the final conductivities in the permeate tank were measured at 8.51, 3.56, and 0.153 mS cm⁻¹, respectively (as listed in Table 5).

The wetting behaviors could be controlled by surfactant adsorption on the membrane surface, which is related to the physical properties of the surfactants. As listed in Table 2, the surfactants used in this study exhibit different molecular weights, surface tensions, hydrophilic-lipophilic balance (HLB) values, and CMCs. The presence of surfactants lowers the surface tension of the medium rapidly [33–35]. Based on the Laplace-Young equation, LEP decreases with decreasing surface tension of liquid, resulting in higher tendency of membrane wetting [36]. However, Span 20 caused a slower membrane wetting rate than Tween 20 despite its lower surface tension. Hence, it seems that surface tension was not the determining factor for the time for onset of wetting and the extent of wetting. On the other hand, all these three surfactants have the same length of hydrophobic tails (12 alkyl units). Thus, the effect of different molecular weights of the surfactants is mainly attributed to the difference in their hydrophilic heads. Moreover, the dominant driving force for the surfactant adsorption is the hydrophobic effect (the tendency of the surfactant to escape from the aqueous environment), which is related to the hydrophobic/hydrophilic properties and CMC of the surfactants [31]. Therefore, the different wetting rates of these surfactants may be mainly attributed to the difference in HLB and CMC among surfactants. As listed in Table 2, Span 20, Tween 20, and SDS have HLB values of 8.6, 16.7, and 40, respectively. The higher the surfactant's HLB value, the more hydrophilic it is [37]. In

other words, a surfactant with a lower HLB value will be more lipophilic and thus be easily adsorbed on a hydrophobic surface due to the hydrophobic effect [32]. Therefore, Span 20 and Tween 20 with relatively lower HLB values caused earlier wetting than the more hydrophilic SDS.

According to literature, surfactant adsorption on hydrophobic surfaces is non-cooperative, as they do not form micelles on the surfaces. Instead, the surfactant unimers form a monolayer [31]. For non-ionic surfactants such as Span 20 and Tween 20, the adsorption on the hydrophobic PVDF membrane surface was dominated by hydrophobic interactions [31]. Considering the fact that 0.15 mM Span 20 and Tween 20 exceeded their respective CMC values, it was likely that the adsorbed unimers of Span 20 and Tween 20 tended to distribute more densely and thus stood erected on the PVDF membrane surface as illustrated in Fig. 4 [38]. Even though the alkyl chain length of a Span 20 unimer is the same as that of a Tween 20 unimer, the former has a much smaller hydrophilic head group as compared to the latter as stipulated by their respective HLB values [37]. The larger hydrophilic heads of Tween 20 unimers were able to draw more water towards the membrane pores once these unimers got adsorbed onto the membrane surface. This may explain why earlier wetting and higher conductivity rising rate were observed for the Tween 20 experiment.

In contrast to non-ionic surfactants, both hydrophobic interactions (nonpolar tails) and electrostatic interactions (polar heads) typically play crucial roles in the adsorption of ionic surfactants like SDS. The PVDF membrane surface was negatively charged, thus SDS would have experienced electrostatic repulsion resulting in fewer unimers getting adsorbed onto the membrane surface. On the other hand, being hydrophilic in nature, the SDS unimers would have the tendency to stay in water instead of attaching onto the PVDF membrane surface. As a result, very few SDS unimers would have been adsorbed onto the membrane surface. In addition, the concentration of SDS in the feed solution was much lower than its CMC, suggesting that the unimers tended to be loosely packed even when a certain amount of SDS were adsorbed on the PVDF surface. Due to the low concentration of SDS on the PVDF membrane surface, it was very likely that the adsorbed unimers laid flat on the membrane surface as illustrated in Fig. 4 [38].

As shown in Fig. 3, the permeate flux of the Span 20 experiment remained fairly constant ($13 \text{ kg m}^{-2} \text{ h}^{-1}$) for 7 h even after the occurrence of wetting and then it gradually declined until no flux was observed after 15 h of operation. In the case of Tween 20, a relatively constant flux was observed for 2 h. After which, there was a gradual increase in flux until 5 h of operation indicating membrane wetting and then there was a subsequent decline in flux. The flux reached zero at approximately 10 h. As discussed above, with the adsorption of Tween 20 unimers on the membrane surface, their hydrophilic heads were able to draw more water towards the membrane pores. This resulted in

the increase of permeate flux after the observed onset of wetting. Similar findings were presented in a recent publication [32]. The flux decline in the case of both Span 20 and Tween 20 suggests that membrane fouling indeed took place during the MD process. Since the concentrations of these two surfactants exceeded their respective CMC values, micelles would have formed in the solutions. This might in turn lead to the blockage and closure of the membrane pores after membrane wetting. Moreover, micelles are able to grow from spherical aggregates to elongated ones with an increase of concentration [31]. In comparison to Span 20, more severe fouling was observed in the case of Tween 20 due to pore blockage by the larger micelles of Tween 20. On the other hand, for SDS, a relatively constant flux (approx. $10 \text{ kg m}^{-2} \text{ h}^{-1}$) was observed for 20 h of operation. This is because the concentration of SDS was well below its CMC value and almost no micelle would have formed in the solution. In addition, very few SDS unimers would have adsorbed onto the membrane surface due to the hydrophilic nature of SDS. Thus, the membrane experienced less fouling and the permeate flux remained fairly constant throughout the operation.

The water contact angles of the different surfactant-fouled membranes are listed in Table 5. It can be seen that the hydrophobicity of PVDF membrane decreased after the adsorption of surfactants and the contact angles of 0.15 mM Span 20, Tween 20, and SDS-fouled membranes were 72° , 64° , and 91° respectively. The decrease of PVDF membrane hydrophobicity can be explained by the hydrophobic interactions between the hydrophobic tails of surfactants and the membrane surface. The interactions orientated the hydrophilic head of surfactants facing outwards, causing the membrane surface to be covered by a hydrophilic layer. The contact angle values were in good agreement with the wetting behaviors of the respective surfactants. Since the membrane surface became the most hydrophilic after the adsorption of Tween 20, more of the feed solution was able to flow through the wetted pores and this resulted in the highest permeate conductivity at the end of the operation.

In the industry, it is more common to use a fixed mass ratio of oil/surfactant in emulsions instead of a fixed molar ratio. As such, the effects of surfactant types with fixed mass concentration (50 mg L^{-1}) in the feed were also examined here, as shown in Fig. 5. The time for onset of wetting for the cases of 50 mg L^{-1} of Span 20, Tween 20, and SDS were ~ 100 min, ~ 130 min, and ~ 140 min, respectively (as listed in Table 5).

By changing the experiment condition from fixed molar concentration to fixed mass concentration of surfactants, the amount of surfactant unimers changed. At a concentration of 50 mg L^{-1} , the molar concentration of Span 20 remained similar (0.144 mM), while molar concentrations of Tween 20 and SDS decreased (to 0.041 mM) and increased (to 0.173 mM), respectively, as compared with the case of 0.15 mM. Therefore, the amount of unimers also affected the wetting and fouling behaviors in addition to the HLB and CMC effects as discussed above. In

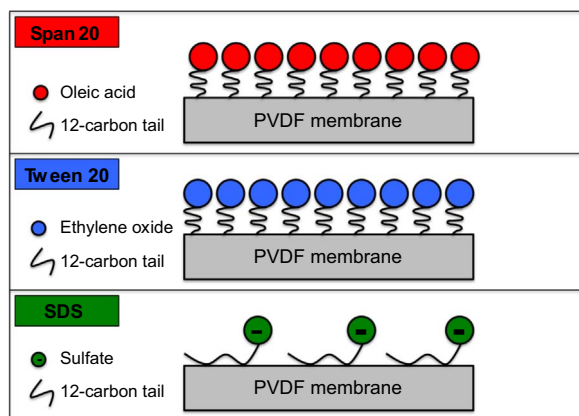


Fig. 4. Illustration of the adsorption of surfactant unimers on the PVDF membrane surface.

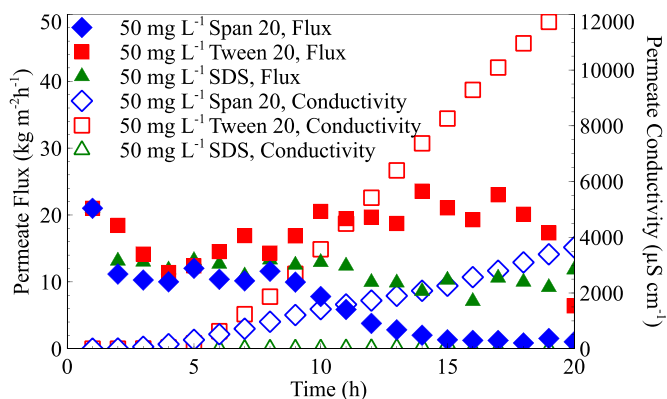


Fig. 5. Effects of surfactant types (same mass concentration) on permeate flux (filled symbols) and conductivity (hollow symbols). ($Q_i=0.7 \text{ L min}^{-1}$; $Q_p=0.25 \text{ L min}^{-1}$; $T_r=333 \text{ K}$; $T_p=293 \text{ K}$).

both 50 mg L^{-1} and 0.15 mM cases, the concentrations of Span 20 were similar. Hence, the fouling and wetting behaviors were similar. In the case of 50 mg L^{-1} Tween 20, relatively fewer unimers in the feed solution resulted in less fouling and delayed onset of wetting in comparison to the 0.15 mM case. Since there was less fouling, the diffusion of NaCl was not as restricted as in the case of 0.15 mM Tween 20. This resulted in a higher final conductivity in the permeate. In the case of 50 mg L^{-1} SDS, more SDS unimers were available to be adsorbed onto the membrane surface, making the membrane surface more hydrophilic. The contact angle values (as listed in Table 5) provided confirmation on this. Their hydrophilic heads were able to draw more water from the feed into the permeate. Therefore, the onset of wetting was brought forward and the final conductivity in the permeate was higher than that of the 0.15 mM SDS case.

3.3. Effects of the presence of oils

The effects of the presence of oil droplets on the permeate flux and conductivity are shown in Fig. 6. It was observed that the extents of membrane fouling and wetting were different when using Tween 20 and Tween 20-stabilized petroleum emulsion as feed. When only 50 mg L^{-1} Tween 20 was present, wetting started to occur at $\sim 130 \text{ min}$ while the onset of wetting was delayed by 30 min in the case of the 1000 mg L^{-1} Tween 20-stabilized petroleum emulsion. As proposed above, in the case of Tween 20, the hydrophobic tails might be attached onto the PVDF membrane surface due to hydrophobic interaction while the hydrophilic ethylene oxide heads might be arranged towards the aqueous solution. These hydrophilic heads had good affinity to water, resulting in faster wetting of the membrane.

As for the Tween 20-stabilized petroleum emulsion, more alkyl tails of the surfactant were bounded with the oil droplets, thus fewer free surfactant unimers were adsorbed on the membrane surface. Therefore, the onset of wetting was delayed in comparison to the Tween 20 case. At the same time, with the prolonged operation time, more and more oil droplets were adsorbed onto the membrane surface due to its hydrophobicity. This caused some pores to be blocked and resulted in a gradual decline of the permeate flux. The accumulation of oil droplets formed a fouling layer that restrained the NaCl diffusion through the wetted pores of the membrane and a slower permeate conductivity rising rate was observed throughout the experiment. The results suggest that even though surfactants have a higher affinity for hydrophobic surfaces than hydrocarbons in general, oil does contribute to membrane fouling.

3.4. Effects of different surfactant-stabilized petroleum emulsions

Three 500 mg L^{-1} surfactant-stabilized petroleum emulsions were

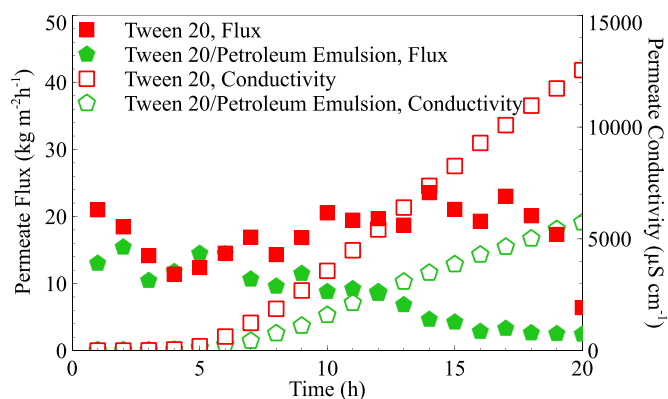


Fig. 6. Effects of the presence of oils on permeate flux (filled symbols) and conductivity (hollow symbols). Tween 20 concentration was 50 mg L^{-1} . Tween 20-stabilized petroleum emulsion was prepared using 50 mg L^{-1} of Tween 20 and 950 mg L^{-1} of petroleum. ($Q_f=0.7 \text{ L min}^{-1}$; $Q_p=0.25 \text{ L min}^{-1}$; $T_f=333 \text{ K}$; $T_p=293 \text{ K}$).

prepared at oil/surfactant mass ratio of 9/1 using Span 20, Tween 20 and SDS. The effects of these surfactant-stabilized petroleum emulsions on membrane fouling and wetting were investigated and the results are presented in Fig. 7. It can be observed that the extent of permeate flux decline was in the sequence of Tween 20 < Span 20 < SDS, suggesting that the SDS-stabilized petroleum emulsion caused the most severe membrane fouling followed by Span 20 and Tween 20. The membrane fouling in these cases might be ascribed to the adsorption of surfactants and oil droplets on the membrane surface and/or pores as well as pore blockage by the foulants. A hypothesis on the interactions between the surfactant-stabilized petroleum emulsions and the hydrophobic PVDF membrane surface is proposed and illustrated in Fig. 8.

The added concentration of Tween 20, 50 mg L^{-1} , was above its CMC at 333 K (3.5 mg L^{-1}) and thus, micelles were formed in the feed solution. The Tween 20 unimers would have stood erected on the PVDF membrane surface to form a monolayer due to hydrophobic interactions. After the adsorption of Tween 20 unimers on the membrane surface, the hydrophilic heads orientated towards the feed solution. Hence, the PVDF membrane surface became more hydrophilic, which in turn promoted more severe pore wetting but restrained the adsorption of oil droplets on the membrane surface [39].

Similar to the Tween 20 case, the Span 20 unimers also formed a monolayer on the PVDF membrane surface due to hydrophobic interactions. As evidenced by the contact angles of the surfactant-fouled membranes presented in Table 5, the Span 20-adsorbed surface is less hydrophilic than the Tween 20 one, and thus relatively more oil droplets might be adsorbed on the membrane surface, aggravating the membrane fouling. In addition, micelles existed in the feed solution and resulted in partial pore blockage since the Span 20 concentration (50 mg L^{-1}) was higher than its CMC (1.6 mg L^{-1}). It was hypothesized that both the oil droplet adsorption and membrane pore blockage by Span 20 micelles led to the more significant flux decline compared with the case of Tween 20-stabilized emulsion. On the other hand, the membrane fouling restrained the diffusion of NaCl to the permeate side.

Due to the hydrophilic nature of SDS, relatively less SDS unimers were adsorbed onto the PVDF membrane as discussed previously in Section 3.2. Therefore, the membrane surface was the least hydrophilic as evidenced by the contact angle of the SDS-fouled membrane shown in Table 5. Hence, the oil droplets had a higher tendency to be attached onto membrane surface, resulting in a more severe fouling. Due to the adsorption of more surfactant-stabilized oil droplets on membrane, the hydrophilic head of SDS might attract more feed to pass through the membrane, which resulted in a relatively more severe increase of the permeate conductivity. Despite the more severe fouling caused by the SDS-stabilized emulsion, the NaCl diffusion was surprisingly faster than the case of the Span 20-stabilized emulsion. The reason for this phenomenon is unclear and further investigation is needed in the future study.

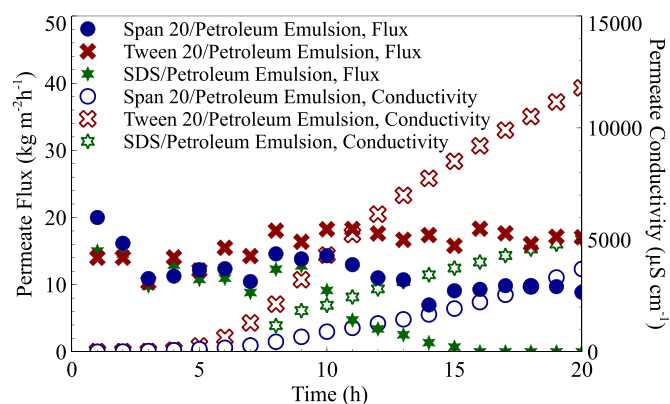


Fig. 7. Effects of different surfactant-stabilized petroleum emulsions on permeate flux (filled symbols) and conductivity (hollow symbols). ($Q_f=0.7 \text{ L min}^{-1}$; $Q_p=0.25 \text{ L min}^{-1}$; $T_f=333 \text{ K}$; $T_p=293 \text{ K}$).

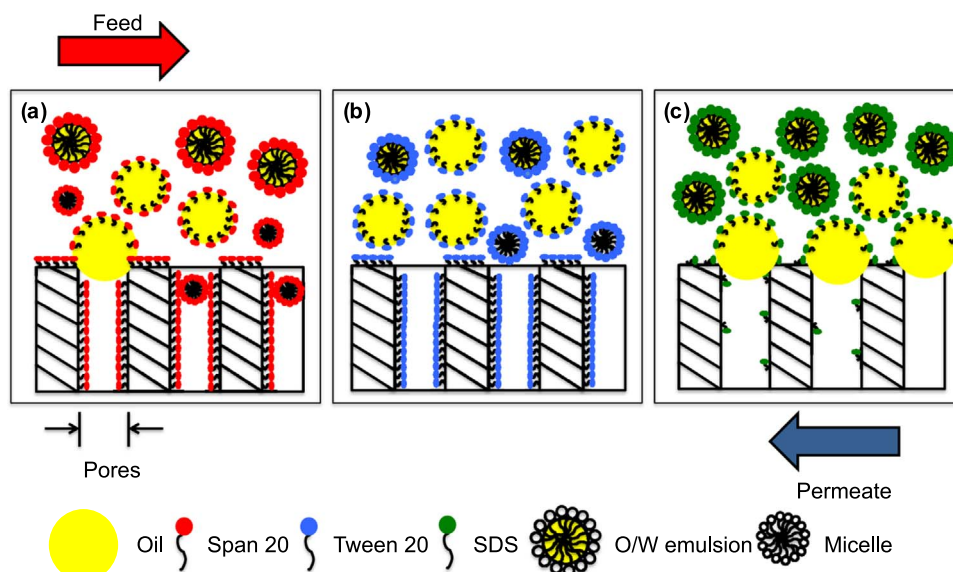


Fig. 8. Proposed interactions of (a) Span 20-stabilized, (b) Tween-20 stabilized, and (c) SDS-stabilized emulsions with the PVDF membrane surface.

3.5. Effects of oil concentration

500, 600 and 1000 mg L⁻¹ Tween 20-stabilized petroleum emulsions were prepared to study the effects of oil concentration on the permeate flux and conductivity. The mass concentration of Tween 20 was fixed at 50 mg L⁻¹ and the mean oil droplet sizes of the different emulsions were kept similar as listed in Table 4. The results are shown in Fig. 9. It is evident that the increase in oil concentration led to more serious fouling, as represented by the more severe decline in permeate flux. With the increase of oil concentration, more oil droplets were adsorbed onto the membrane surface and caused membrane pore blockage. Thus, a more significant decrease of the permeate flux was observed. Similarly, the trend observed in the permeate conductivity was as expected. Wetting became slower when more oil droplets blocked the membrane pores. The results suggest that MD could be an effective option for recovering water from produced water at low oil concentration.

3.6. Effects of oil types

The effects of Tween 20-stabilized VPO emulsion on the permeate flux and conductivity are shown in Fig. 10. Generally, petroleum oil includes paraffins (15–60%), naphthenes (30–60%), aromatics (3–30%), and asphaltics while VPO contains heavy distillates with relatively higher boiling points that are hardly volatile. In comparison

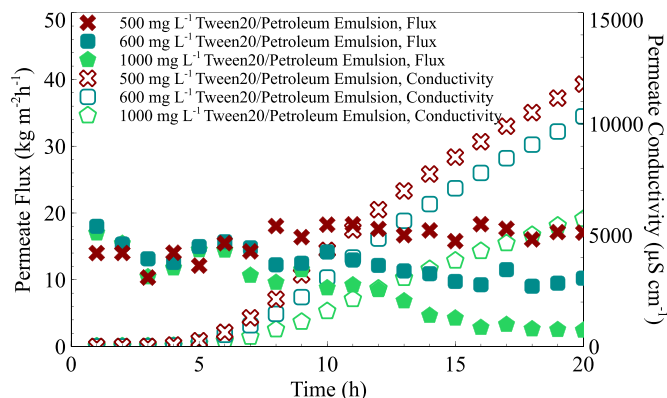


Fig. 9. Effects of oil concentration on permeate flux (filled symbols) and conductivity (hollow symbols). ($Q_f=0.7$ L min⁻¹; $Q_p=0.25$ L min⁻¹; $T_f=333$ K; $T_p=293$ K).

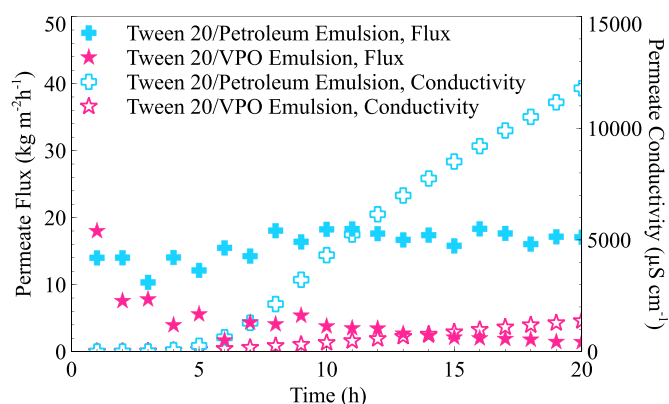


Fig. 10. Effects of oil types on permeate flux (filled symbols) and conductivity (hollow symbols). ($Q_f=0.7$ L min⁻¹; $Q_p=0.25$ L min⁻¹; $T_f=333$ K; $T_p=293$ K).

with the Tween 20-stabilized petroleum emulsion, more severe fouling was observed for the VPO emulsion. This is believed to be ascribed to the higher proportions of heavy hydrocarbons present in VPO [39]. This suggests that MD could be considered for water recovery from produced water containing higher proportions of lighter hydrocarbons.

3.7. Confirmation of surfactant penetration into membrane pores and membrane fouling

It was hypothesized that pore wetting leads to an increase in permeate conductivity as presented in Table 5. In order to validate this, penetration of surfactants into the membrane pores were verified using the ATR-FTIR characterization test on the inner surfaces of the wetted PVDF membranes. The FTIR spectra of the pristine and wetted PVDF membranes were plotted against that of pure Span 20, Tween 20, and SDS, as presented in Fig. 11.

As shown in Fig. 11 (a), Span 20 has three characteristic peaks: the 2853 cm⁻¹ and 2920 cm⁻¹ peaks were attributed to CH₂ symmetric and asymmetric stretching respectively, while the broad peak around 3389 cm⁻¹ was assigned to O-H stretching. These peaks were only observable on the wetted PVDF membranes but were undetected on the pristine PVDF membrane, demonstrating the presence of Span 20 on the inner surfaces of the wetted PVDF membranes. Similar results were also observed for membranes wetted in the case of both Tween 20 and SDS. The FTIR spectra coupled with the rise in permeate conductivity

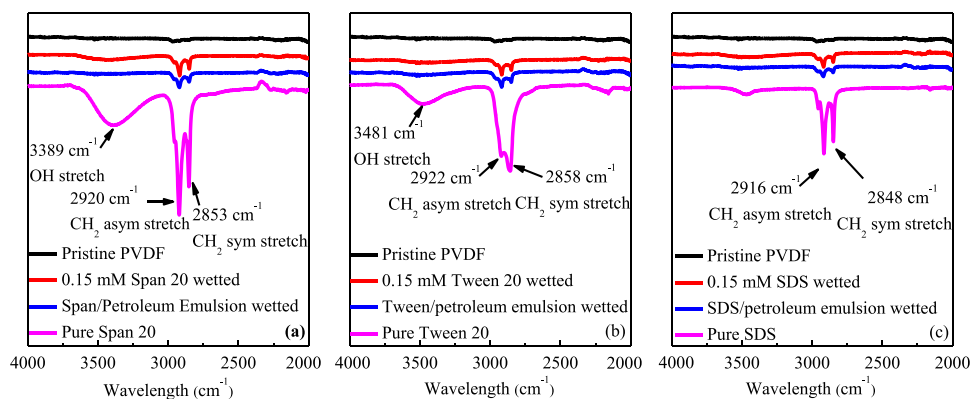


Fig. 11. FTIR spectra of the pristine and wetted PVDF membranes. Transmittance normalized against CF peak. (a) Span 20 experiments, (b) Tween 20 experiments, (c) SDS experiments.

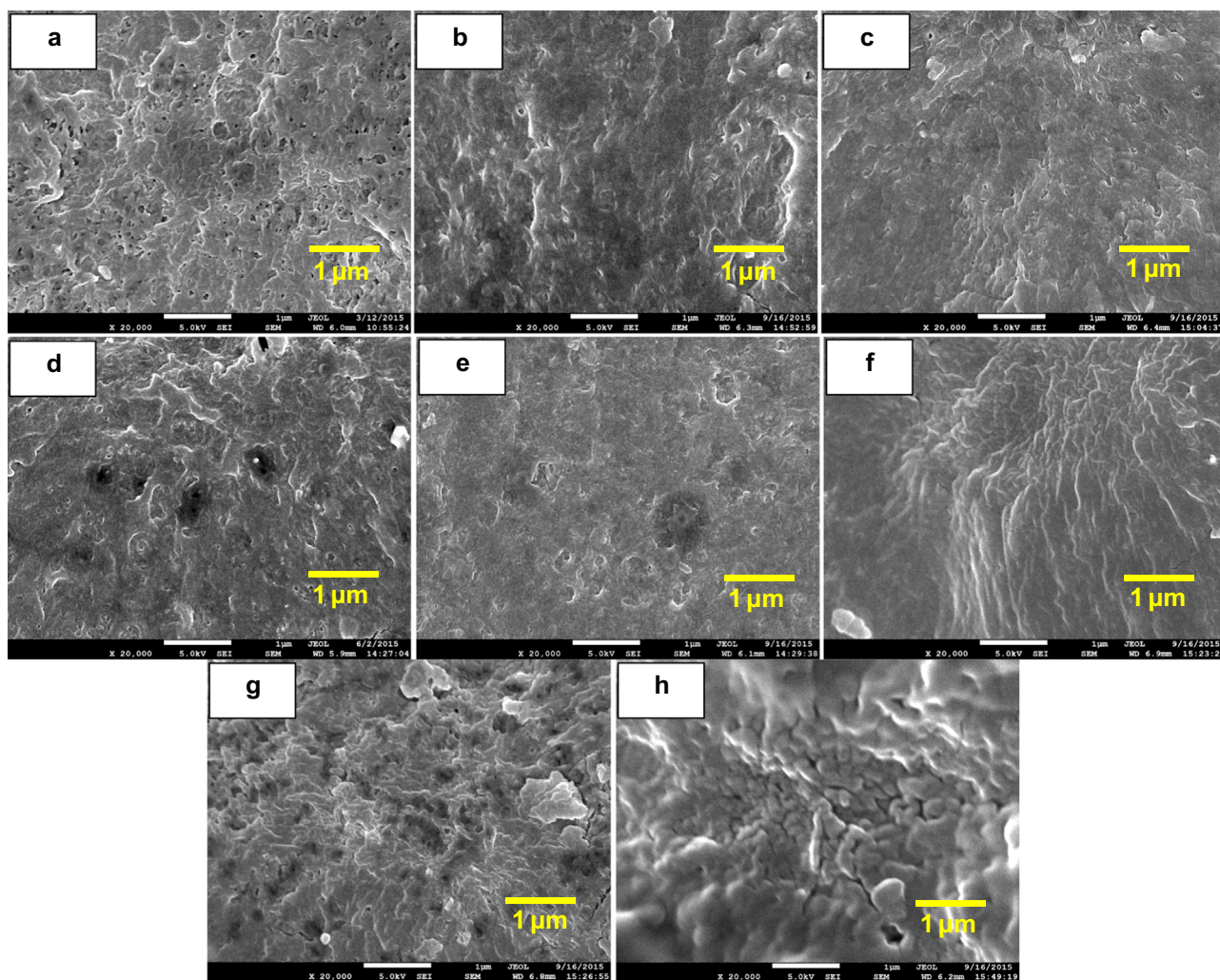


Fig. 12. SEM images of (a) pristine PVDF membrane and membranes fouled by (b) 50 mg L^{-1} Span 20, (c) 50 mg L^{-1} Tween 20, (d) 50 mg L^{-1} SDS, (e) 500 mg L^{-1} Tween 20/Petroleum Emulsion, (f) 500 mg L^{-1} Span 20/Petroleum Emulsion, (g) 500 mg L^{-1} SDS/Petroleum Emulsion, and (h) 500 mg L^{-1} Tween 20/VPO Emulsion.

in all experiments were indicative of the occurrence of membrane wetting.

The outer surface morphologies of the pristine and fouled PVDF membranes were characterized using SEM and the images are shown in Fig. 12. Abundant pores could be clearly observed on the pristine PVDF membrane. However, the membrane surfaces were covered by foulants

after the MD experiments no matter which type of feed solution was used. As shown in Fig. 12 (e) and (h), the oil foulant layer formed by the Tween 20-stabilized VPO emulsion seemed denser than the layer formed by the Tween 20-stabilized petroleum emulsion, demonstrating the more severe membrane fouling caused by VPO emulsion as discussed in Section 3.6.

4. Conclusions

This study attempts to provide an in-depth understanding of the relationship between different surfactant-stabilized O/W emulsions and the hydrophobic PVDF membrane surface in DCMD. The results reveal that the time for onset of wetting for different surfactants were dependent on their HLB values. A surfactant with lower HLB value tended to be adsorbed more on the membrane surface and caused an earlier onset of wetting.

The presence of oils in the emulsion delayed the onset of wetting of the membrane. Fouling was observed to be less severe for emulsions stabilized by surfactants with a lower HLB value. The severity of membrane fouling increased with increasing oil concentration. Moreover, membrane fouling caused by the VPO emulsion was also more severe due to the higher proportions of heavy hydrocarbons in VPO. These results suggest that MD should be considered as an option for recovering water from produced water with lower oil concentration and higher proportions of lighter hydrocarbons.

This study revealed that robust membranes with better anti-fouling and anti-wetting properties are required to eliminate or minimize the issues of fouling and wetting. These findings suggest that membrane surface modification is required to achieve anti-fouling and anti-wetting properties. This, coupled with process optimization, is expected to advance DCMD as an economically viable technology for treating produced water. These proposed works will be done in our future study.

Acknowledgements

This work was funded by the Johnson Matthey Technology Centre. We also acknowledge funding support from the Singapore Economic Development Board to the Singapore Membrane Technology Centre.

References

- [1] T.D. Rangarajan, B. Ali Heydari, and H. Amr, State of the Art Treatment of Produced Water, Water Treatment, InTech, 2013.
- [2] A. Fakhru'l-Razi, A. Pendashteh, L.C. Abdullah, D.R.A. Biak, S.S. Madaeni, Z.Z. Abidin, Review of technologies for oil and gas produced water treatment, *J. Hazard. Mater.* 170 (2–3) (2009) 530–551.
- [3] IEA, World Energy Outlook 2013, 2013, p. 700.
- [4] A. Alkhudhiri, N. Darwish, N. Hilal, Produced water treatment: application of air gap membrane distillation, *Desalination* 309 (2013) 46–51.
- [5] A. Hong, A.G. Fane, R. Burford, Factors affecting membrane coalescence of stable oil-in-water emulsions, *J. Membr. Sci.* 222 (1–2) (2003) 19–39.
- [6] A.S.C. Chen, J.T. Flynn, R.G. Cook, A.L. Casaday, Removal of oil, grease, and suspended solids from produced water with ceramic crossflow microfiltration, *SPE Prod. Eng.* 6 (2) (1991) 131–136.
- [7] S.H.D. Silalahi, T. Leiknes, Cleaning strategies in ceramic microfiltration membranes fouled by oil and particulate matter in produced water, *Desalination* 236 (1–3) (2009) 160–169.
- [8] A. Motta, C. Borges, K. Esquerre, A. Kiperstok, Oil produced water treatment for oil removal by an integration of coalescer bed and microfiltration membrane processes, *J. Membr. Sci.* 469 (2014) 371–378.
- [9] D. Ali, M.M. Husein, T.G. Harding, Produced water treatment by micellar-enhanced ultrafiltration, *Environ. Sci. Technol.* 44 (5) (2010) 1767–1772.
- [10] D. Wandera, S.R. Wickramasinghe, S.M. Husson, Modification and characterization of ultrafiltration membranes for treatment of produced water, *J. Membr. Sci.* 373 (1–2) (2011) 178–188.
- [11] D. Wandera, H.H. Himstedt, M. Marroquin, S.R. Wickramasinghe, S.M. Husson, Modification of ultrafiltration membranes with block copolymer nanolayers for produced water treatment: the roles of polymer chain density and polymerization time on performance, *J. Membr. Sci.* 403–404 (2012) 250–260.
- [12] P. Xu, J.E. Drewes, Viability of nanofiltration and ultra-low pressure reverse osmosis membranes for multi-beneficial use of methane produced water, *Sep. Purif. Technol.* 52 (1) (2006) 67–76.
- [13] S. Mondal, S.R. Wickramasinghe, Produced water treatment by nanofiltration and reverse osmosis membranes, *J. Membr. Sci.* 322 (1) (2008) 162–170.
- [14] N. Tomer, S. Mondal, D. Wandera, S.R. Wickramasinghe, S.M. Husson, Modification of nanofiltration membranes by surface-initiated atom transfer radical polymerization for produced water filtration, *Sep. Sci. Technol.* 44 (14) (2009) 3346–3368.
- [15] L. Ning, L.X. Li, B. McPherson, R. Lee, Removal of organics from produced water by reverse osmosis using MFI-type zeolite membranes, *J. Membr. Sci.* 325 (1) (2008) 357–361.
- [16] M. Melo, H. Schluter, J. Ferreira, R. Magda, A. Júnior, O. de Aquino, Advanced performance evaluation of a reverse osmosis treatment for oilfield produced water aiming reuse, *Desalination* 250 (3) (2010) 1016–1018.
- [17] B.D. Coday, P. Xu, E.G. Beaudry, J. Herron, K. Lampi, N.T. Hancock, T.Y. Cath, The sweet spot of forward osmosis: treatment of produced water, drilling wastewater, and other complex and difficult liquid streams, *Desalination* 333 (2014) 23–35.
- [18] Y. Liao, R. Wang, A.G. Fane, Fabrication of bioinspired composite nanofiber membranes with robust superhydrophobicity for direct contact membrane distillation, *Environ. Sci. Technol.* 48 (11) (2014) 6335–6341.
- [19] D.L. Shaffer, L.H. Arias Chavez, M. Ben-Sasson, S.R.-V. Castrillón, N.Y. Yip, M. Elimelech, Desalination and reuse of high-salinity shale gas produced water: drivers, technologies, and future directions, *Environ. Sci. Technol.* 47 (17) (2013) 9569–9583.
- [20] A. Alkhudhiri, N. Darwish, N. Hilal, Membrane distillation: a comprehensive review, *Desalination* 287 (2012) 2–18.
- [21] M. Gryta, K. Karakulski, Application of membrane distillation for the concentration of oil-water emulsions, *Desalination* 121 (1) (1999) 23–29.
- [22] M. Gryta, K. Karakulski, A.W. Morawski, Purification of oily wastewater by hybrid UF/MD, *Water Res.* 35 (15) (2001) 3665–3669.
- [23] D. Singh, K.K. Sirkar, Desalination of brine and produced water by direct contact membrane distillation at high temperatures and pressures, *J. Membr. Sci.* 389 (2012) 380–388.
- [24] G. Zuo, R. Wang, Novel membrane surface modification to enhance anti-oil fouling property for membrane distillation application, *J. Membr. Sci.* 447 (2013) 26–35.
- [25] S. Zhang, P. Wang, X. Fu, T.-S. Chung, Sustainable water recovery from oily wastewater via forward osmosis-membrane distillation (FO-MD), *Water Res.* 52 (0) (2014) 112–121.
- [26] Y. Wu, S. Iglauer, P. Shuler, Y. Tang, W.A. Goddard, Alkyl polyglycoside-sorbitan ester formulations for improved oil recovery, *Tenside Surfactants Deterg.* 47 (5) (2010) 280–287.
- [27] P.M. Kruglyakov, *Hydrophile - Lipophile Balance of Surfactants and Solid Particles: physicochemical aspects and applications*, Elsevier Science, Amsterdam, The Netherlands, 2000.
- [28] X. Yang, R. Wang, L. Shi, A.G. Fane, M. Debowski, Performance improvement of PVDF hollow fiber-based membrane distillation process, *J. Membr. Sci.* 369 (1–2) (2011) 437–447.
- [29] Y. Liao, R. Wang, M. Tian, C. Qiu, A.G. Fane, Fabrication of polyvinylidene fluoride (PVDF) nanofiber membranes by electro-spinning for direct contact membrane distillation, *J. Membr. Sci.* 425–426 (2013) 30–39.
- [30] L.L. Schramm, *Surfactants: fundamentals and Applications in the Petroleum Industry*, The Press Syndicate of the University of Cambridge, United Kingdom, 2000.
- [31] B. Kronberg, K. Holmberg, B. Lindman, *Surface Chemistry of Surfactants and Polymers*, John Wiley & Sons, United Kingdom, 2014.
- [32] P.-J. Lin, M.-C. Yang, Y.-L. Li, J.-H. Chen, Prevention of surfactant wetting with agarose hydrogel layer for direct contact membrane distillation used in dyeing wastewater treatment, *J. Membr. Sci.* 475 (2015) 511–520.
- [33] A.C.M. Franken, J.A.M. Nolten, M.H.V. Mulder, D. Bargeman, C.A. Smolders, Wetting criteria for the applicability of membrane distillation, *J. Membr. Sci.* 33 (3) (1986) 315–328.
- [34] C. Boo, J. Lee, M. Elimelech, Omniphobic polyvinylidene fluoride (PVDF) membrane for desalination of shale gas produced water by membrane distillation, *Environ. Sci. Technol.* 50 (22) (2016) 12275–12282.
- [35] C. Boo, J. Lee, M. Elimelech, Engineering surface energy and nanostructure of microporous films for expanded membrane distillation applications, *Environ. Sci. Technol.* 50 (15) (2016) 8112–8119.
- [36] L.D. Tijing, Y.C. Woo, J.-S. Choi, S. Lee, S.-H. Kim, H.K. Shon, Fouling and its control in membrane distillation—a review, *J. Membr. Sci.* 475 (0) (2015) 215–244.
- [37] P. Walstra, *Physical Chemistry of Foods*, Marcel Dekker, Inc, New York, 2001.
- [38] F. Tiberg, J. Brinck, L. Grant, Adsorption and surface-induced self-assembly of surfactants at the solid–aqueous interface, *Curr. Opin. Colloid Interface Sci.* 4 (6) (1999) 411–419.
- [39] D. Lu, T. Zhang, J. Ma, Ceramic membrane fouling during ultrafiltration of oil/water emulsions: Roles played by stabilization surfactants of oil droplets, *Environ. Sci. Technol.* 49 (7) (2015) 4235–4244.